Construction and Building Materials 359 (2022) 129511

Contents lists available at ScienceDirect

Construction and Building Materials

journal homepage: www.elsevier.com/locate/conbuildmat

Development of a dry mortar with nanosilica and different types of industrial waste for the application in borehole heat exchangers

C. Castán-Fernández [a], G. Marcos-Robredo [a], M.P. Castro-García [a,*], M.A. Rey-Ronco [a], T. Alonso-Sánchez [b]

[a] Departament of Energy, University of Oviedo, Oviedo, Spain
[b] Departament of Mining Exploitation and Prospecting, University of Oviedo, Oviedo, Spain

ARTICLE INFO

Keywords:
Geothermal backfill material
Geothermal grout
Industrial waste
Industrial by-products
Borehole Heat Exchanger (BHE)
Nanosilica

ABSTRACT

A geothermal borehole is a heat exchanger between the soil and a heat transfer fluid. This fluid flows throw in the geothermal pipes, which has been inserted into borehole. Using a Ground Source Heat Pump (GSHP) systems, the fluid provides heating and cooling buildings.

The space between the geothermal pipes and the ground is filled with a geothermal backfill. This geothermal fill must be having high thermal conductivity for facilitate the heat flow. In this way this fill is an important element in a Borehole Heat Exchanger as its choice can result in significant economic and energy savings during the geothermal installation's lifetime. However, in general it has not received enough attention.

The geothermal backfill materials formed by a mixture of cement, fine aggregate, sand and/or additions are known as geothermal grouts. The aggregated additives and the other materials aggregated confers to the geothermal backfill high thermal conductivity. This property is rejected in the conventional grouts used in buildings.

On the other hand, the use of industrial waste or by-products in geothermal grouts is considered more sustainable, for it reduces landfill volume and the need of exploiting new mineral resources.

This paper describes the development of a geothermal grout, named MG 7. MG-7 has improved thermal properties compared with conventional grouts. In this case, mining and by-products from surrounding companies have been used, following the principles of the circular economy.

To determinate the geothermal grout properties different techniques and conventional equipment has been used. However, to calculate the thermal conductivity a specific device developed by the authors. Finally, it has been obtained a pre-dosed geothermal grout with a thermal conductivity of 2.01 ± 0.08 W/m•K (K = 2), in which 30 % of the aggregates come from industrial waste, such as mine tailings, ladle furnace slag, fly ash and silica fume. It also contains 2 % of silica nanoparticles.

1. Introduction

Due to the increase in the price of fossil fuels, to the social rejection of nuclear power and to the effects of global warming, several countries have begun to look for new energy resources. Recently, geothermal energy has become an unquestionable protagonist, especially the so-called Ground Source Heat Pump (GSHP) systems.

The main advantage of the GSHP systems is their undemanding geological conditions, thus these energy resources can be used by means of Borehole Heat Exchanger (BHE), almost throughout the whole territory. Moreover, it is a sustainable and very efficient energy with remarkable energy savings. Fig. 1 represents the geothermal borehole with the geothermal probes for the fluid flows and the location of the geothermal backfill.

Generally geothermal backfill has been divided into:

- Geothermal backfill has been based on drill cuttings
- Geothermal backfill has been based on bentonite
- Geothermal backfill has been based on cement, Philippacopoulos and Berndt (2001) [1].

Using drill cutting backfills has the advantage of lowest installation costs (Jin *et al.*, 2019 [2]) The objective of this study is to develop a

* Corresponding author.
E-mail address: castromaria@uniovi.es (M.P. Castro-García).

https://doi.org/10.1016/j.conbuildmat.2022.129511
Received 31 May 2022; Received in revised form 9 September 2022; Accepted 16 October 2022
Available online 26 October 2022

Nomenclature

Symbols

b	Addition
c	Cement
k	Coefficient of Permeability [m/s]
r	Admixture
s	Aggregate
sp	Superplasticizer
w	Water

Greek letters

λ	Thermal Conductivity [W/m•K]

Abbreviations

AAS	Atomic Absorption Spectrometry
BA	Bottom ash
BHE	Borehole Heat Exchanger
CDW	Construction and Demolition Waste
CLSM	Controlled Low-Strength Material
FA	Fly Ash
FT	Fluorspar tailings
GSHP	Ground Source Heat Pump
HDPE	High Density Polyethylene
ICP-OES	Inductively Coupled Plasma Optical Emission Spectrometry
LFS	Ladle Furnace Slag
NS	Nanosilica
NTU	Nephelometric Turbidity Units
PCM	Phase Change Material
PVC	Polyvinyl Chloride
SEM	Scanning Electron Microscopy
SF	Silica Fume
SS	Silica Sand
THW	Transient Heat Wire
TRT	Thermal Response Test
WHO	World Health Organization
XRD	X-ray Diffraction
XRF	X-ray Fluorescence

geothermal grout based on cement with improved thermal properties used the selected additives.

The geothermal grout is pumped, from the bottom to the top, into the borehole after the geothermal pipes have been introduced. With this pumped the geothermal grout acquired a special fluidity property and setting time. The geothermal grout must fill all the gaps to prevent pore formation, because those pores reduced thermal conductivity.

The area where the present study is developed is Asturias (Spain). Traditionally, its economy was based on mining, metallurgy and energetic industries. Asturias faces to two problems: the crisis in those sectors and the high amount and type of waste generated. Moreover, the use of waste is also a challenge for our society, who increasingly promotes its recovery to minimize, as much as possible, its environmental impact.

In Asturias you can find:

- a mining company (MPD Fluorspar, Minersa Group) with a mineral processing plant, dedicated to the exploitation of fluorite deposits.
- a coal-fired power plant with pulverized coal combustion (EDP Group) and a coal-fired power plant with circulating fluidized bed combustion (Hunosa Group).
- a metallurgical company which generates waste such as ladle furnace or silica fume, also used in this work.

For this study different products have been used, according to circular economy principles:

- queues laundry mining from MDP Fluorspar, Minersa Group, mining company dedicated to the exploitation of fluorite deposits.
- Fly ash from energetic companies:

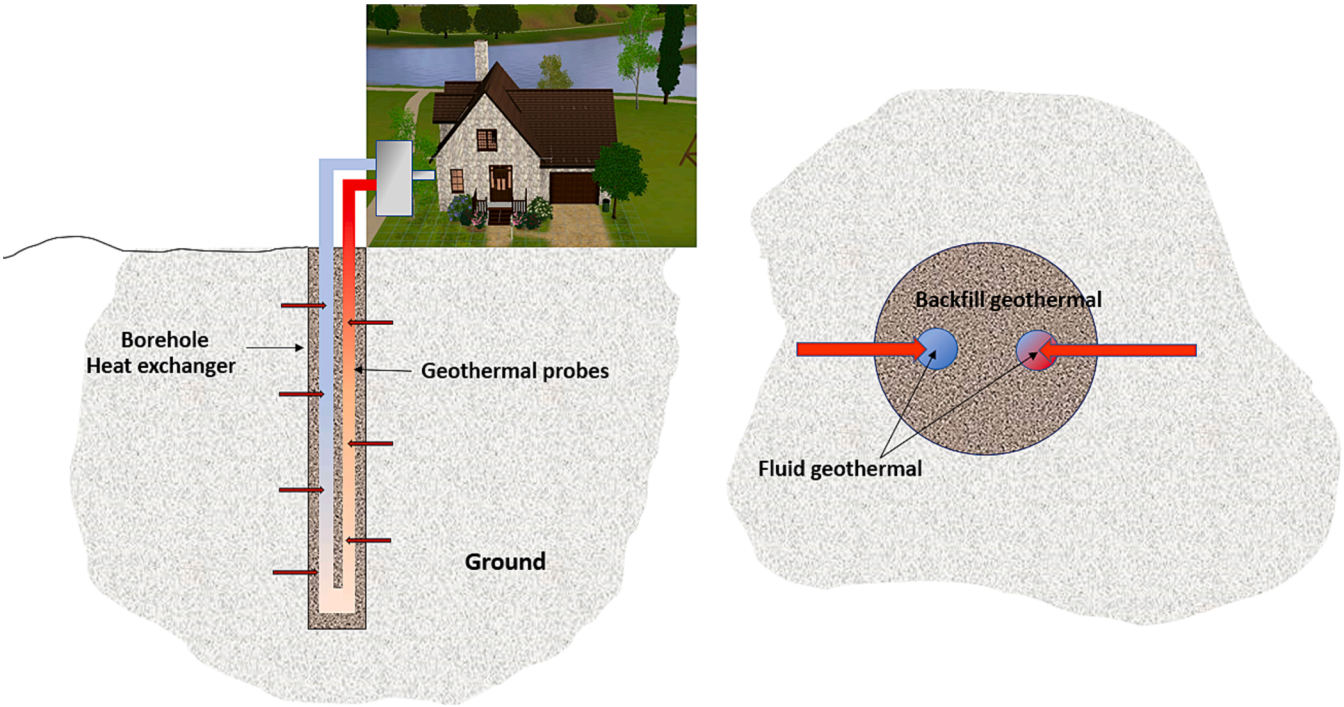

Fig. 1. Borehole Heat Exchanger (BHE) and geothermal backfill location.

- o EDP Group: a coal-fired power plant with pulverized coal combustion
- o Hunosa Group: a coal-fired power plant with circulating fluidized bed combustion

- Ladle furnace slag or silica fume, from metallurgic company Arcelor Mittal.

A dry mortar (pre-dosed geothermal grout) in which nanosilica, fluorspar tailings and ladle furnace slag, are used along with other materials, is developed. The main innovation is the employment of nanosilica, which beneficially modifies the properties of the geothermal grout.

1.1. Geothermal grout properties

According to Indacoechea *et al.,* 2015 [3] and Sáez Blázquez *et al.*, 2017 [4], the geothermal backfill material of a BHE must fulfil the following:

I. Allow the heat exchange between ground and carrier fluid, with the aim of gaining the maximum heat transmission.
II. Cause a hydraulic barrier to avoid the connexion between two or more aquifers.
III. Protect the borehole wall.

In order to meet those requirements, the geothermal backfill material must have appropriate properties, in relation to thermal conductivity, compressive strength, permeability, consistence, bleeding, linear shrinkage, durability and not creating environmental impact (Hellström G., 2011 [5] and Allan M.L., 2015 [6]).

Backfiĺs thermal conductivity establishes the heat flow, in this way, is an important property of the geothermal backfill materials. In the case of using a geothermal grout, this property depends on several factors, as:

- water-cement ratio: Daehoon *et al.*, 2017 [7] showed a decrease in thermal conductivity of a cement-based grout when increasing the water/cement (w/c) ratio.
- sand ratio: Allan M.L., 2015 [6] and Daehoon *et al.*, 2017 [7] found that thermal conductivity increases when the amount of sand in the grout material increases.
- Particles' shape: According to Côte *et al.*, 2005 [8] the value of effective thermal conductivity decreased when the shape of the particles were rounded instead of angular.
- Types of aggregates: Borinaga Treviño *et al.*, 2012 [9] noted that by adding aggregates to cement, thermal conductivity improves, although the type of aggregate was more important than the proportion. The silica has a high thermal conductivity. So, the best materials to mix with the cement must be those whose have a high ratio of silica. Anotherwise, the bentonite, was the most useful backfill in boreholes due to its waterproof properties but its thermal conductivity is lower than silica.

The thermal conductivity's geothermal borehole is inversely proportional to the thermal resistance's borehole. The thermal resistance is defined as the heat Exchange between the ground and the heat carrier fluid. The value of thermal resistance value is determined by the Thermal Resistance Test (TRT). This test can only be done once the borehole is in operation. The TRT determined the joint effect of the thermal conductivity backfill and of the well work of the borehole.

According to Sanner B., 2011 [10] the geological materials borehole's had a within range of thermal conductivity values. Those values were lower than metallic materials' values. For example, quartzite had a high thermal conductivity, of the order of 5.5 [W/m K], limestone 2.8 [W/m K], sandstone 2.3 [W/m K] or clay 0.5 [W/m K].

Several authors proposed to use geothermal grouts with a thermal conductivity near to 2 [W/m·K], so the thermal resistance's borehole might be 0.070 [m·K /W]. Lee *et al.* (2010) [11] proposed for most grounds' thermal conductivities range between 1.7 and 2.1 W/m•K. Sanner *et al.* (2003) [12] said that raising thermal conductivity to 2.5 [W/m·K] produced a thermal resistance's borehole improvement of only 0.010 [m·K /W]. In other way, using a geothermal grout with a thermal conductivity of 0.8 [W/m·K] produced a thermal resistance of 0.140 [m·K /W].

It proved the low influence between the thermal conductivity's pipes and the thermal resistance's borehole. For this reason, the most used material is high density polyethylene (HDPE) because its low cost, easy installation and low corrosion, even its low thermal conductivity (0.4 W/m•K).

Permeability and consistency are other important properties of geothermal backfill materials. According to Young Sang *et al.*, 2020 [13] the consistency of geothermal backfill materials measured in a flow table, according to UNE-EN 1015–6 [14], should be bigger than 20 cm. Meanwhile, it is desirable that permeability has a low value. However, Erol and François., 2014 [15] concluded that to avoid the formation of cracks, geothermal backfill materials should not have extremely low permeability values.

Also, the geothermal grout setting time must not be lower than 3 h for allowing the easily pumped into the borehole. A conventional geothermal borehole has a diameter of ± 150 mm, a depth of 150 m and pumping injection rate around 20 L/min. Workability time is reduced if it is minor to 3 h, optimum time between 3 and 12 h, tolerable time between 12 and 24 h and elevated time if it is over 24 h.

After finishing the pumped grout, this one must be toughened as soon as possible to resist the thrust of the ground and to minimize the dragging of fresh grout, due to the hydraulic communication between aquifers or the circulation that could be produced by a pump located in the vicinity.

On the other hand, the grain size and the w/c ratio are important elements to consider when choosing the geothermal backfill materials.

- Thus, in order to ensure good pumpability and appropriate workability, Pascual Muñoz *et al.*, 2018 [16] limited the maximum grain size to 2 mm.
- According to Allan, M.L. (2015) [6], the increase of w/c ratio, as well as the reduction of the thermal conductivity, has also other consequences, such as linear shrinkage rise, bleeding, permeability or the reduction of compressive strength and durability. Also Indacoechea *et al.*, 2015 [3] stated that, the w/c ratio and the permeability coefficient are inversely proportional to both the thermal conductivity and mechanical strength.

1.2. Geothermal grouts types

Allan y Philippacopoulos (2000) [17] reported that before year 2000 in USA was used cement and backfills based on bentonite whose thermal conductivity values were near to 0.8 W/m•K, due to their low permeability (Montaser *et al.*, 2021 [18]). In the case of the cement, due also to its elevated mechanical strength. Nevertheless, both cement and bentonite had the problem of low thermal conductivity high shrinkage under dry conditions. Previously it was used silica sand due to its low cost Dehdezi *et al.* (2011) [19].

Several publications were written about the improvement grout properties using different types of additives:

- Allan M.L., 1996 [20]; Allan and Kavanaugh S.P., 1999 [21] and Berndt M.L. [22] and Philippacopoulos A.J., 2001 [1] analyzed the influence of steel fiber in the geothermal grout. It was determined:

  - an improvement in thermal conductivity's geothermal grouts (2.64 W/mK),
  - density and mechanical resistance increase,
  - decrease consistence's geothermal grouts.

- Other additives used are from metallurgic or energetic industries. Adding blast furnace slag to a Portland cement grout with silica sand, water and plasticizer, improves thermal conductivity to values of 2.2 W/mK (Allan M.L.,1997 [23]). This addiction produced a light improves in compressive strength (Berndt M.L., 2010 [24]). By adding fly ashes to cement grout the same improvement in thermal conductivity is observed Allan M.L., 1997 [23]. Borinaga Treviño *et al.*, 2012 [9] used EAF slag in a Porland type CEM II cement grout with water, additives and superplasticizer. This addition produced a thermal conductivity value of 1.5 W/m•K. If they used Construction and Demolition Waste (CDW) instead of EAF the thermal conductivity value was 0.2 W/mK less. In this way, if they used silica sand instead of EAF the thermal conductivity value was 0.6 W/mK more. If they used limestone sand instead of EAF the thermal conductivity value was 0.3 W/mK more. Any of these additives led to an improvement in the thermal conductivity of the base, which was only 0.9 W/mK. Borinaga Treviño *et al.*, 2013 [25] measured the thermal conductivity in a mixture of CEM III Portland cement, water, BOF converter slag, EAF slag and a small proportion of bentonite, which was 0.90 W/m•K. Variations in the value of thermal conductivity were detected by substituting the BOF converter slag for RCD (1.16 W/mK). However, replacing both slag and RCD by silica sand seems more interesting because increased the value of thermal conductivity to 1.61 W/mK. Young Sang *et al.*, 2020 [26] assessed the properties of several CLSM, in which, water, cement, fly ashes, sand and iron and steel slag were used. Tan Manh *et al.*, 2020 [27] had compared conventional geothermal backfill with different mixtures of CLSM (silica sand, cement, water and fly ashes).
- Berndt M.L., 2010 [24] determined that using microsilica slightly decreased the permeability coefficient. Sáez Blázquez *et al.*, 2017 [4] analyzed different geothermal grouts using calcium aluminate cement with silica sand and they obtained a thermal conductivity value of 2.45 W/mK but added aluminum shavings the value of thermal conductivity increased to 2.79 W/mK.
- Lee *et al.*, 2010 obtained that added graphite to the bentonite grout the thermal conductivity value was 3.5 W/mK. Delaleux *et al.*, 2012 [28] and Erol and François, 2014 [15] used natural graphite for improving the thermal conductivity of bentonite grouts. Borinaga Treviño *et al.*, 2013 [25] measured the thermal conductivity of a commercial grout mixture of bentonite, Portland type CEM III cement, water and graphite, obtaining values of 1.05 W/mK. Pascual Muñoz *et al.* 2018 [16] and Indacoechea., 2015 [1] used graphite in cement geothermal grouts.
- Other additives that have been studied come from the mining industry. So Alrtimi *et al.* (2013) [29] prepared a cement-based grout using fluorspar and pulverized fuel oil ashes, obtaining a thermal conductivity of 2.88 W/m•K in the mixture. Young Sang *et al.*, 2018 [26] used cement, tailings from a gold mine and silica sand, achieving a thermal conductivity of 1.57 W/m•K. Dequan *et al.*, 2020 [30] used tailings from a gold mine They also prepared geothermal backfills by mixing the laundry tailings from the iron mine with loess. Recently, nanotechnology has been progressively introduced in the construction industry. The addition in concretes of nanoparticles such as nanoalumina, nanoiron and especially nanosilica has been widely investigated. However, no references about the use of nanosilica in geothermal grouts has been found in scientific literature.

As a summary, one of the most used geothermal grout is Mix 111, which has the following properties (Allan M.L. and Philippacopoulos A. J., 1999 [21]):

- Water-cement ratio equal to 0.55
- Permeability of $1.6{\cdot}10^{-12}$ m/s
- Compressive strength 36,70mpa at 28 days
- Flexural strength of 6.35 mpa at 56 days
- Adhesion stress to the geothermal pipe of 150 kpa
- Thermal conductivity of 2.16 W/mK. with a decreased in thermal resistance of 29 to 35 % compared to the use of a bentonite backfill.
- the thermal resistance of the borehole is reduced by 29 to 35 % compared to the use of a bentonite filler (Allan and Philippacopoulos., 1999 [21]).

2. Materials and methods

In this section the materials used for preparing the samples, the selection of the specific grout and the tested done are shown. To obtain the definitive grout the next steps had been followed:

1. Analyzed the properties of the materials and selection of the optimal ones. In this step, 30 mixtures were prepared and preliminary tested were done.
2. From the 30 previous samples, the best 7 ones were selected to make thermal tests.
3. The best geothermal grout was selected to make a complete analysis.

2.1. Samples preparation

The materials used come from the studio environment. These, their origin and abbreviations are summarized in the Table 1.

The industrial waste used were selected for two reasons: nearby to the studio environment and its optimal properties for the geothermal grout.

- Silica sand was used because of its high thermal conductivity. Moreover, its angular pebbles confers high waterproof and high mechanical resistance.
- Construction and Demolition Waste derive from concrete where the barren's concrete is silica and it improve the thermal conductivity.
- Fly ashes and bottom ashes were selected from:
  - o Aboño Power Plant (Asturias). Silica type: mullite and quartz minerals.
  - o La Pereda Power Plant (Asturias). Calcareous type: mullite, quartz, anhydrite (CaSO4), and illite.
- Fluorite queues laundry had been selected for its high silica rate and for its crystal structure because that improved heat exchange Callister W.D., 2007 [31].
- Ladle furnance slag were selected because of its crystal structure.
- Microsilica use improved the sulfate resistance and mechanical resistance, also reduced the permeability, the exudation and the segregation.

Aggregates chemical composition according to suppliers is shown in Table 2.

The granulometric analysis of the aggregates with the biggest grain size (BA, FT, CDW y SS) was performed with an AS 300 Retsch electromagnetic sieve shaker, in accordance with UNE-EN 933–1 [32]. The grain-size distribution obtained is shown in Table 3, where it can be observed that the maximum size of BA, CDW and SS is 2 mm, whereas for the FT is 0.5 mm.

For aggregates with lower grain size (FA, LFS and SF) a HELOS/RODOS Sympatec Laser Diffraction instrument was used. Before the granulometric analysis, the samples were dried in a drying oven at 105 °C.

The grain-size distribution obtained with the laser diffraction instrument is shown in Table 4. It can be observed that the aggregate with a smaller size is SF, where 99.04 % is<60 μm and 18.05 % has a size lower than 1.80 μm.

Table 1
Materials used in geothermal grouts. Abbreviations and origin.

Type	Symbol		obs	abbreviation	Type	Origin
Cement	c	Portland		CEMI	EN 197–1 CEM I 42.5 R	Tudela Veguín cement
aggregate	s	Biggest grain size	artificial aggregates	SS	silica sand	Cantera Grado S.L.
				CDW	Construction and Demolition Waste	Reciclajes de Santiago S.L.
				LP-BA	bottom ash	Pereda Thermal Power Plant of Hunosa GroupAboño Thermal Power Plant (EDP Group)
				A-BA		
				FT	Fluorspar tailings	Mineral processing plant "Mina Ana" (Minersa Group)
		Lower grain size		LP-FA	fly ash	Pereda Thermal Power Plant of (Hunosa Group).Aboño Thermal Power Plant (EDP Group)
				A-FA		
				LFS	ladle furnace slag	ArcelorMittal
				SF	silica fume	FerroAtlántica
addition	b			SB	bentonita sódica	Sepiolsa del grupo Minersa
				NS	pyrogenic nanosilica AEROSIL® 200	Evonik Industries
admixture	r	superplasticizer		sp	MasterCast 205 MA	Master Builders Solutions
water	w				Drinking water	

Table 2
Aggregates Chemical composition (percentage).

	SiO2	Al_2O_3	Fe_2O_3	*CaO*	*MgO*	*BaO*	SO_3	*MnO*	Na_2O	K_2O	TiO_2
CEM I	19.79	5.69	3.47	63.57	0.92		2.63		0.14	0.78	
BA	45.6	23.9	4.47	10.14	2.11		1.87	0.11	0.98	3.29	0.49
FT	71.23	1.03	1.39	7.89	0.11	0.36	2.48	0.01	0.02	0.35	
CDW	58.39	16.41	2.79	5.16	1.49		1.61	0.11	2.11	3.79	0.29
SS	93.34	3.04	2.31	0.01	0.01			0.01	0.02	0.04	
LP-FA	46.1	23.1	4.23	10.31	1.81		4.91	0.09	0.57	3.16	0.41
A-FA	51.84	23.99	10.58	4.85	1.43		0.30	0.06	0.83	2.29	1.03
LFS	24.17	4.11	0.99	59.87	2.83			0.27	0.01	0.01	0.37
SF	95.11	0.41	1.23	0.16	0.31		0.15	0.11	0.25	0.39	0.01
SB	57.91	23.07	5.83	0.59	1.49		0.10	0.03	3.26	0.46	0.37
NS	99.80	0.05									0.03

Table 3
Grain-size distribution of BA, FT, CDW and SS.

Sieve size [mm]	Passing percentage (%)			
	BA	FT	CDW	SS
2	100.00	100.00	100.00	100.00
1	82.36	100.00	82.08	73.64
0.5	53.36	100.00	56.60	31.72
0.25	20.04	98.76	29.12	5.40
0.125	11.28	52.84	16.76	3.04
0.063	4.80	24.68	13.04	1.00

Table 4
Grain-size distribution of FA, LFS and SF.

Particle size [μm]	Passing percentage (%)		
	FA	LFS	SF
122	100.00	100.00	100.00
60	90.46	88.00	99.04
30	72.79	61.08	94.93
15	51.99	31.12	87.62
7.40	26.18	10.76	71.34
3.60	11.35	4.35	40.85
1.80	4.92	2.05	18.05

2.1.1. First phase of sample preparation and selection

Initially, 30 samples were prepared with different materials and dosages, as is shown in the Table. 5.

Firstly, a qualitative analysis of workability, exudation and cracking were done on these 30 samples. Then the workability time and the simple compressive strength as a function of the proportion of mixing water, were analyzed.

The grout workability during the kneading process and exudation in the samples after 3 h of the kneading process have been evaluated. The shrinkage, cohesion, and cracking were assessed at 28 days. These properties can be evaluated a naked eyed.

The sample mechanical resistance was measured at the first day. It was used a pocket penetrometer to determine if the simple compressive strength was ±1 N/mm^2. It was measured in the first day because is the minimum value of compressive resistance that a stone has, according to ISRM, 1981 [33].

2.1.2. Second phase of sample preparation and selection

From the previous phase, 7 samples had been selected. With them some rectangular prisms (180 mm × 70 mm × 50 mm) were prepared for a deeper study (Fig. 2). The name and materials used in the 7 geothermal grouts candidates are shown in Table 5.

The mixture proportions, in weight, of the 7 candidates are shown in Table 6. Each sample is formed by a mixture of aggregates. The main aggregate (s_1) is the one with the highest percentage.

Samples MG 1, MG 2 and MG 3 contain 100 % of artificial aggregate. In MG 1, MG 2, MG 3 and MG 4 the main aggregates are each of the four aggregates with the biggest grain size: BA, FT, CDW and SS, respectively. Samples MG 5, MG 6 and MG 7 combine SS and FT, as they are the pair of aggregates that should have highest thermal conductivity, based on their mineralogical composition.

The mixture proportions of the 7 candidates were obtained performed by searching a continuous grain size and high compactness. The grading curves were adjusted to the Fuller curves, with the aggregate maximum sizes of 0.5 mm for sample MG 2 and of 2 mm for the rest. Moreover, previous tests were performed in which the dosage of the superplasticizer was determined for a maximum w/c ratio of 0.55 and a

Table 5
Samples prepares.

Name	Materials				Dosage		
	Cement c	Arid s	Addition b	Additive r	s/c	b/c	r/c
M 11	c	BA	…	sp	1.00	…	0.01
M 12	c	BA	…	sp	2.00	…	0.01
M 13	c	BA	…	sp	2.50	…	0.01
M 14	c	FT	…	sp	1.00	…	0.01
M 15	c	FT	…	sp	2.00	…	0.01
M 16	c	FT	…	sp	2.50	…	0.01
M 17	c	CDW	…	sp	1.00	…	0.01
M 18	c	CDW	…	sp	2.00	…	0.01
M 19	c	CDW	…	sp	2.50	…	0.01
M 20	c	SS	…	sp	1.00	…	0.01
M 21	c	SS	…	sp	2.00	…	0.01
M 22	c	SS	…	sp	2.50	…	0.01
M 23	c	LP-FA	…	sp	0.20	…	0.01
M 24	c	LP-FA	…	sp	0.10	…	0.01
M 25	c	LP-FA	…	sp	0.03	…	0.01
M 26	c	A-FA	…	sp	0.20	…	0.01
M 27	c	A-FA	…	sp	0.10	…	0.01
M 28	c	A-FA	…	sp	0.03	…	0.01
M 29	c	LFS	…	sp	0.20	…	0.01
M 30	c	LFS	…	sp	0.10	…	0.01
M 31	c	LFS	…	sp	0.03	…	0.01
M 32	c	NS	…	sp	0.20	…	0.01
M 33	c	NS	…	sp	0.10	…	0.01
M 34	c	NS	…	sp	0.03	…	0.01
M 35	c	…	BS	sp	…	0.20	0.01
M 36	c	…	BS	sp	…	0.10	0.01
M 37	c	…	BS	sp	…	0.03	0.01
M 38	c	…	NS	sp	…	0.20	0.01
M 39	c	…	NS	sp	…	0.10	0.01
M 40	c	…	NS	sp	…	0.03	0.01

Fig. 2. Geothermal grout candidates.

mixing time of <5 min.

This maximum rate based on the data described by Allan and Philippacopoulos., 2000 [17] was selected and then confirmed by essays at the research laboratory.

The quantity of mixing water, for the all the samples, is the necessary for achieving mixtures with fluid consistency (>200 mm, in accordance with ASTM C940-98a [34].

A planetary mixer (ICON) with a 5-litre capacity was employed to make the samples. Subsequently, samples were placed in a chamber at 20 °C and 95 % of relative humidity, and they were removed from the moulds 48 h later after being mixed. Then, they were placed, to curate, in a water bath for 7 days.

Before performing the tests, samples were placed into the drying oven at 60 °C for 5 days, and then they were left at room temperature for 48 h, so the samples temperatures and room temperature were in balance.

The thermal conductivity of the 7 geothermal grouts candidates was determined after performing tests with a homemade apparatus, developed by the research team. The apparatus is based on the Transient Hot Wire (THW) method whose mathematical basis is the Infinite Linear Source (ILS) model. The apparatus consists of a nichrome hot wire (Cronix 80-E, 0,2 mm diameter and 0–510 mm length), an adjustable direct current power supply TENMA 72–10480 (0-3A) (0–30 V) which is able to supply a maximum power of 90 W, a temperature sensor (K-type thermocouple OMEGA Engineering), placed parallel at 1 mm from the hot wire. The datalogger consists of a thermocouple connector, a 14-Pin amplifier (AD595AQ, from Analog Devices) and a microcontroller board (Arduino Uno, *R*3 version) connected to a PC via a USB cable. It has a relative precision of 5 % and a relative accuracy of 3 %. (Fig. 3).

The apparatus is reliable, economical, lightweight, easy to construct and easy to use. Equipment is adapted to the range of conductivities to be measured and sample size. It has high precision. However, there are already commercial equipment that perform these functions.

The thermal conductivity of the specimen can be determined knowing the heating power q per unit length, which dissipates the linear heat source and measuring temperature evolution, applying the Equation [1] (Castán-Fernández *et al.*, 2018 [35]).

$$T\ (r,t) - \ T_0 = \ \frac{q}{4\cdot\pi\cdot\lambda}\cdot E_1\left[\frac{r^2}{4\cdot\alpha\cdot t}\right] \tag{1}$$

where,

- q heat per unit length $\frac{W}{m}$. determined by knowing the electrical current I of the linear heat source, its length L and the voltage drop ΔV along it.
- T_0 Initial temperature, equal with room temperature at the beginning of the study.
- $T(r,t)$ temperatures measured from the beginning of heating and at a radial distance r from the linear heat source
- λ thermal conductivity tested, $\frac{W}{(K\cdot m)}$.
- α themal difusivity tested , $\frac{m^2}{s}$
- E_1 integral exponential function

Table 6
Mixture proportions of the 7 geothermal grouts candidates. AA artificial aggregate, c = CEM I, b = NS y r = sp.

Sample	% AA	Mixture proportions [kg/kg]							
		s_1/c	s_2/c	s_3/c	s_4/c	s_5/c	b/c	w/c	r/c
MG 1	100	0.90 (BA)	0.03 (FA)	0.05 (LFS)	0.02 (SF)	—	0.02	0.46	0.01
MG 2	100	1.80 (FT)	0.06 (FA)	0.10 (LFS)	0.04 (SF)	—	0.02	0.54	0.01
MG 3	100	1.80 (CDW)	0.06 (FA)	0.10 (LFS)	0.04 (SF)	—	0.02	0.52	0.01
MG 4	20	1.60 (SS)	0.14 (FA)	0.20 (LFS)	0.06 (SF)	—	0.02	0.44	0.01
MG 5	25	1.50 (SS)	0.10 (FT)	0.14 (FA)	0.20 (LFS)	0.06 (SF)	0.02	0.48	0.01
MG 6	40	1.20 (SS)	0.40 (FT)	0.14 (FA)	0.20 (LFS)	0.06 (SF)	0.02	0.55	0.01
MG 7	30	1.40 (SS)	0.20 (FT)	0.14 (FA)	0.20 (LFS)	0.06 (SF)	0.02	0.50	0.01

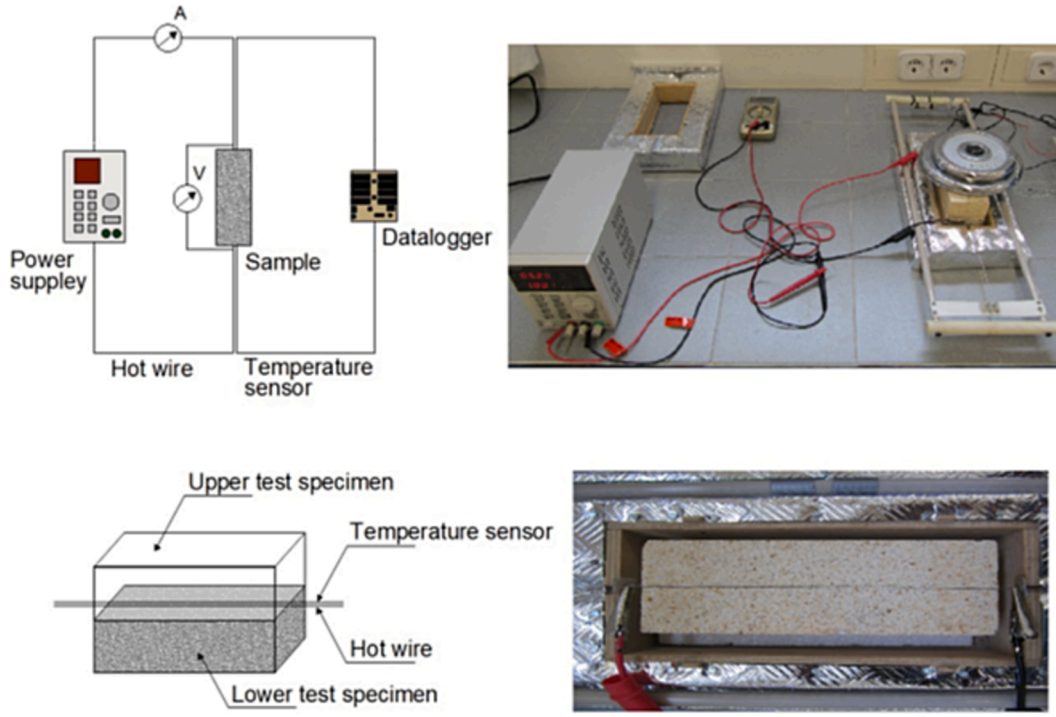

Fig. 3. Diagram and photograph of the measurement equipment.

So, thermal conductivity λ is obtained.

Power per unit length of hot wire with values between 6 W/m had been used, for low conductivities, and 100 W/m, for high conductivities, with heating times lower than an hour. These two conditions guaranteed not reaching excessively high temperatures.

Three thermal conductivity tests were performed on each sample, taking the average as the result. The tests were performed at room temperature, as it is the regular working temperature of geothermal grouts. Specifically, room conditions were 15–25 °C temperature and a relative humidity of 55–65 %.

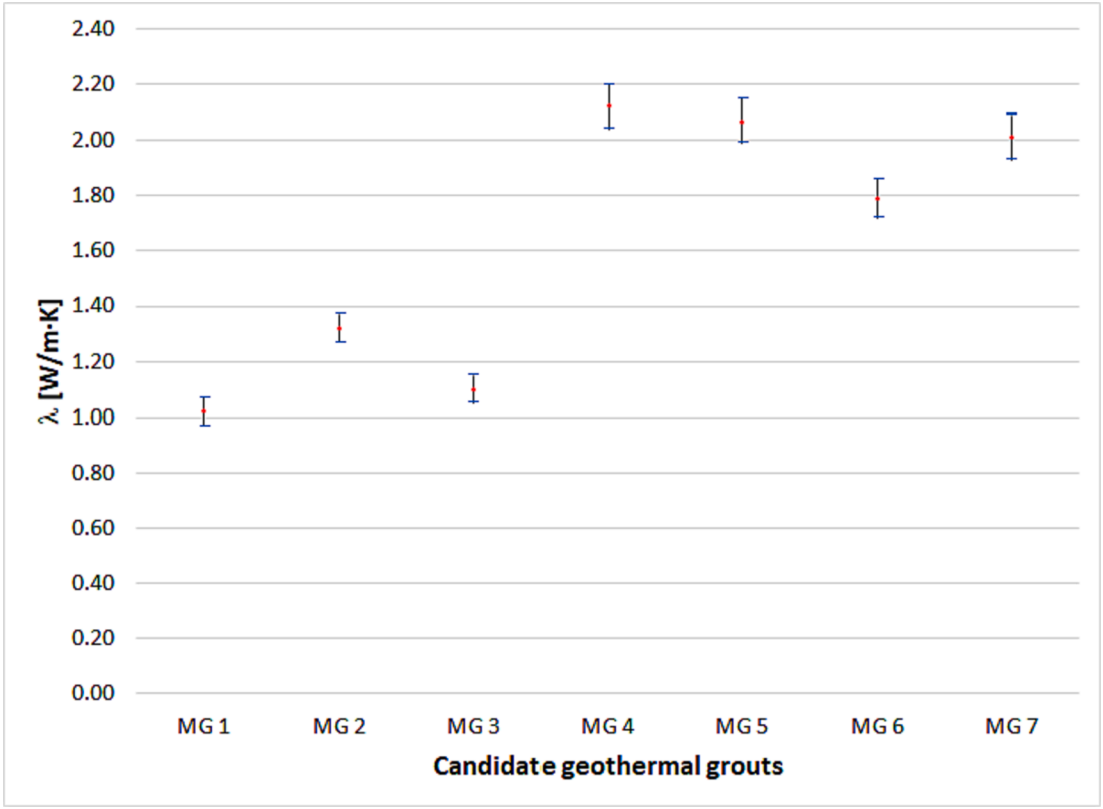

Fig. 4. Confidence intervals of the thermal conductivity of the 7 geothermal grouts candidates.

The 95 % confidence intervals of the thermal conductivity, corrected from the MCT, are shown in Fig. 4.

As expected, the highest values of thermal conductivity correspond to the samples containing silica sand (MG 4, MG 5, MG 6 and MG 7 respectively). The artificial aggregate percentage and the thermal conductivity of these 4 samples are shown in Fig. 5. It can be noted that the greater the artificial aggregate percentage, the lower the thermal conductivity.

Taking as a reference the geothermal grout with the highest thermal conductivity (MG 4), the thermal conductivities of MG 6, MG 7 and MG 5 are 15.56 %, 5.19 % and 2.36 % smaller, respectively.

2.1.3. *Third phase: Characterization of MG 7*

Finally, MG 7 was chosen as the final geothermal grout (2.01 ± 0.08 W/m•K (K = 2)), which presents a compromise between thermal conductivity and environmental sustainability (percentage of artificial aggregate). In addition, the previously analysed mechanical properties have been considered.

The following set of essays described were realized over sample MG7:

The preparation of the fresh mortar and the test samples were performed following the UNE-EN 1015–2 [36]. Below, the tests carried out to fully characterise MG 7 are listed:

1. The consistency test (UNE-EN 1015–3 [37]) was performed in a manual flow table with a 300 mm diameter (Fig. 6).
2. The setting time (UNE-EN 480–2 [38]) is determined using an automatic Vicat apparatus (Ibertest). The penetrations were performed every 10 min.
3. To estimate the bleeding (ASTM C940-98a [34]) a 1.000 ml graduated cylinder was used, into which 800 ml of fresh mortar was placed. To prevent the evaporation of the bleed water, the test tube was covered with a plastic wrap. Readings were performed every 15 min over 3 h and a pipette was employed to collect the bleed water.
4. The bulk density of the fresh mortar (UNE-EN 1015–6 [39]) was estimated with a precision balance and a metal container of 125 mm diameter and 1 L capacity.

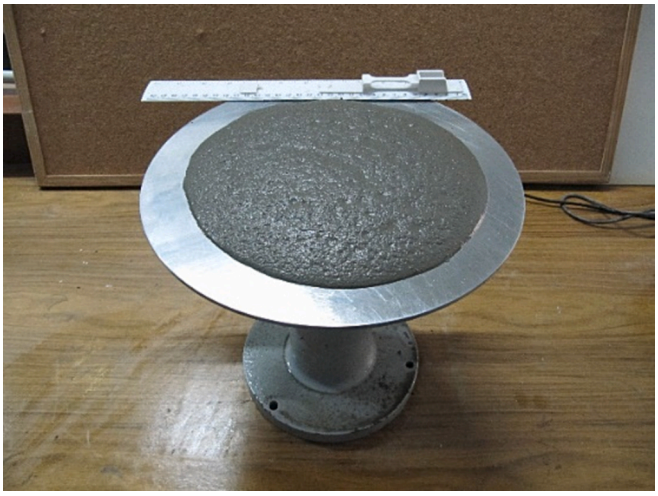

Fig. 6. Consistency test.

5. The dry bulk density of the hardened mortar (UNE-EN 1015–10 [40]) was determined preparing two prismatic test tubes, which were kept for 48 h in a chamber at 20 °C and 95 % of relative humidity. Next, they were unmoulded and introduced into a water bath for 7 days to curate. The sample weights when it was dry (previously placed in a drying oven at 70 °C), wet and submerged were obtained in the hydrostatic balance. Finally, open porosity was determined with these 3 values (UNE-EN 993–1 [32]).
6. The compressive and flexural strength (UNE-EN 1015–11[41]) were derived preparing three prismatic test tubes and stored 2 days in a humid chamber at 20 °C and 95 % of relative humidity. Then, they were unmoulded and placed for 5 days in a water bath and finally they were placed in the humid chamber until day 28. The test tubes were tested at 7th day and at 28th day after being prepared in a universal testing machine of 200 kN, applying the load at a uniform velocity of 50 N/s for the flexural test, and at 400 N/s for the compressive test.

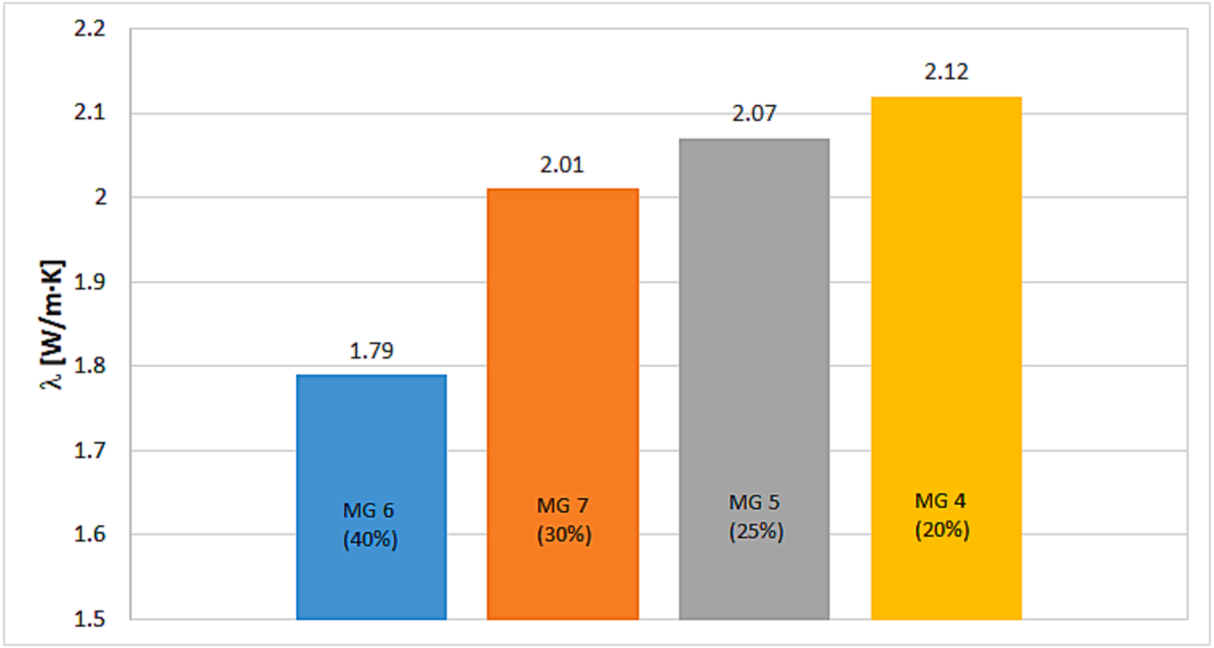

Fig. 5. Thermal conductivity of MG 4, MG 5, MG 6 and MG 7. The percentage represents the artificial aggregate content.

7. The homogeneity study of MG 7 was performed by visually determining its grade of anisotropy and of segregation. For this purpose, a cylindrical test tube is employed, to which a longitudinal cut is given to observe the aggregate particles distribution. The mould (Fig. 7.a) is formed by a split PVC pipe, with 50 cm of length and 5 cm of diameter. The split PVC pipe was unmoulded after 48 h, and the test tube was placed for 7 days in a water bath to curate. The test tube was cut longitudinally after 15 days with a stone cutting circular saw (Fig. 7.b).
8. To measure the linear shrinkage (ASTM C490-07 [42]) 3 prismatic test tubes were prepared, which were stored in a chamber for 7 days at 20 °C and 95 % of relative humidity. Then they were unmoulded and conserved in a cabinet at 20 °C and 50 % of relative humidity. The test lasted 90 days, and the readings were achieved via a length comparator. Readings were performed daily during the first 15 days, and later every week.
9. The permeability coefficient (ASTM D5084-90 [43]) was determined with 2 cylindrical tubes of 76.3 mm of length and 38.1 mm of diameter. These test tubes were stored for 24 h in a chamber at 20 °C and 95 % of relative humidity. Then, they are unmoulded and placed for 15 days in a water bath to curate. Subsequently, the flexible wall permeameter test was performed. For this purpose, a multitest machine (Tritech 100) was employed. A pressure cell is also employed into which the cylindrical test specimen was located. The whole apparatus used during the test is shown in Fig. 8.a. The pressure cell is on the right (Fig. 8.b).
10. The adherence strength between the geothermal grout and the pipe of the BHE was estimated carrying out an experiment, calculating the maximum tangential stress between them with an electromechanical press. This experiment was specifically designed because there is not any normalized experiment for this purpose. Firstly, 32 holes of 3 mm of diameter were made uniformly along a PVC pipe of 110 mm of outer diameter and 120 mm of length. This PVC pipe simulated the geothermal boreholes walls through which water can flow towards the grout. Inside the PVC pipe, a HDPE pipe was placed in a coaxial way. This HDPE pipe has 40 mm of outer diameter, 3.7 mm of thickness and 140 mm of length (Fig. 9.a). This internal pipe simulated the geothermal probe. Both pipes were placed into a container (simulates the ground), and water was poured until the holes of the PVC pipe were covered. The PVC pipe had the function of being the mould (Fig. 9.b).

This experiment was made by Allan and Philippacopoulos., 1999 [44] with grout MIX 111, but without the holes. These holes were considered necessary because they simulate water contact with the grout, thus achieving more realistic setting and hardening conditions.

Then, the fresh mortar was poured, and the container was covered with plastic wrap. The mortar was subjected to conditions of setting and hardening in permanent contact with water, which normally occurs in the field. After 28 days, the plastic wrap was withdrawn, and the mortar-pipe set was removed from the container (Fig. 10.a). Finally, by using an electromechanical press of 100 kN, a vertical load was applied over the coaxial pipe of HDPE until reaching the shear strength (Fig. 10.b). Thus, the maximum tangential stress between the mortar and the HDPE pipe can be calculated.

11. Twenty wet-dry cycles and twenty freeze–thaw cycles were executed to perform the durability study of the hardened mortar. For both tests, 8 prismatic test specimens were stored over 48 h in a chamber at 20 °C and 95 % of relative humidity. Then, they were unmoulded and placed for 15 days in a water bath to curate. In each wet-dry cycle, 3 test tubes were completely immersed over 24 h in a thermostatic bath with water at 15 °C and then, they were introduced into a drying oven for 24 h at 55 °C. In each freeze–thaw cycle, 3 test tubes are used. They were kept in a freezer at a temperature of −18 °C for 24 h and, subsequently, they were immersed for 24 h in a thermostatic bath with water at 15 °C that completely covered them. To evaluate they effects and to determine weight variation of, the emergence of cracks, peeling, fissures or flaking in the test tubes was monitored. Moreover, using an universal testing machine, the compressive and flexural strength test of the 8 test tubes (3 used in the wet-dry cycles, 3 used in the freeze–thaw cycles and 2 that will be used as reference) was performed. Thus, comparing the results obtained in the 8 test tubes, the loss of the geothermal grout mechanical strength when subjected to wet-dry and freeze–thaw cycles can be quantified.
12. The chemical composition of the dry mortar is estimated using an X-ray Fluorescence (XRF) analytical technique. The determination of the main elements of the geothermal grout was performed with the PHILIPS PW2404 sequential spectrometer. Minor and

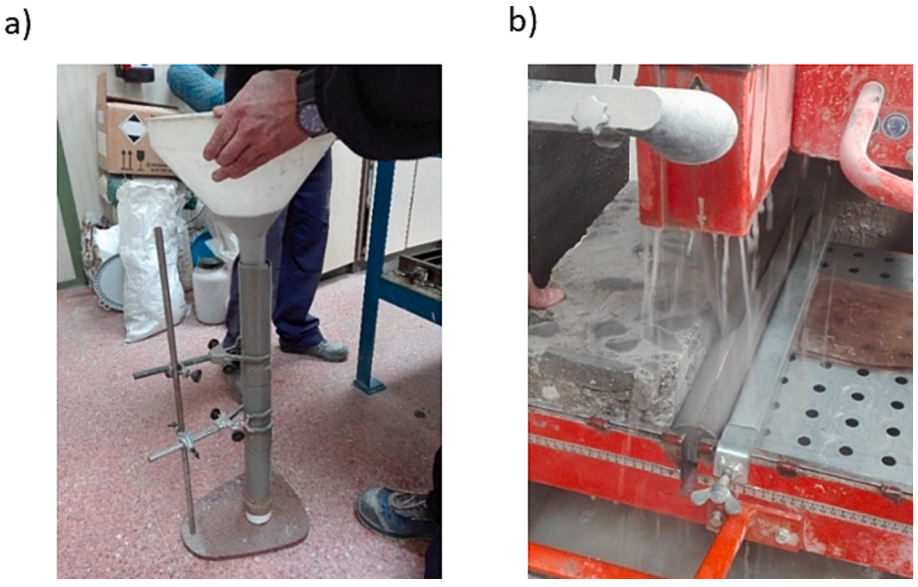

Fig. 7. a) Filling the split PVC pipe. b) Test tube cutting.

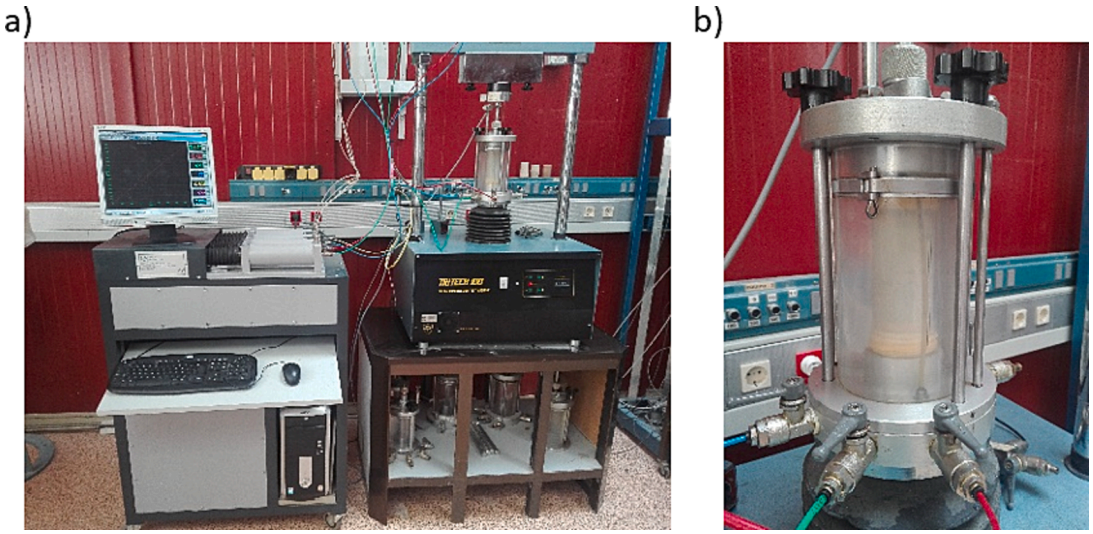

Fig. 8. a) Permeability test. b) Pressure cell with the test tube.

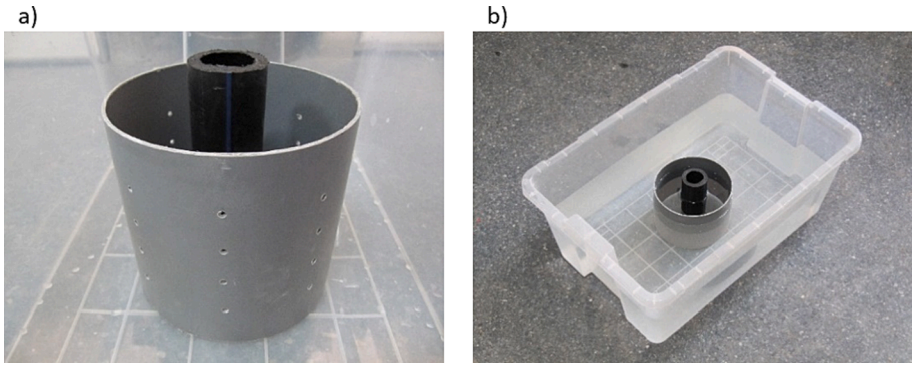

Fig. 9. a) Pipes. b) Container with water.

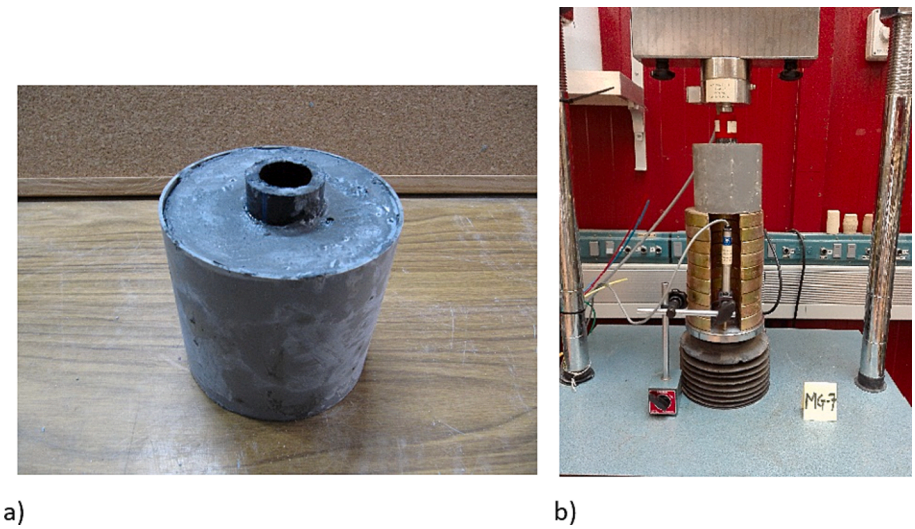

Fig. 10. a) Mortar-pipe set. b) Adherence test.

trace elements were determined with a Niton XL3t analyser (180 s analysis time).

13. The mineralogical analysis of the hardened mortar was performed via X-ray Diffraction (XRD), with a PHILIPS XPERT PRO powder diffractometer.
14. The hardened mortar microstructure was studied with a Scanning Electron Microscopy (SEM), using a JEOL JSM-6610LV scanning electron microscope. This microscope is complemented with an Inca energy-350 microanalysis equipment via Energy Dispersive X-ray Spectroscopy (EDX), with an X-ray detector (X-Max 50).

15. Finally, the environmental impact that the geothermal grout could have in the groundwater was estimated. Based on the corresponding leachate, the pH (UNE-EN ISO 10,523 [45]), electrical conductivity (UNE-EN ISO 10,523 [45]), turbidity (UNE-EN ISO 7027–1 [46]) and chemical analysis were estimated. First, following (UNE-EN ISO 11,885 [47]), a leaching test of a monolithic sample was performed. Four stages (days 3, 7, 30 and 60 respectively) were carried out during the leaching test in a plastic glass, including leaching renewal and eluate collection (water obtained from the leaching test). The pH and electrical conductivity were measured in the 4 stages. Turbidity and the eluate chemical composition were estimated in the last stage. The quantitative determination of the chemical elements: arsenic (As), barium (Ba), cadmium (Cd), cobalt (Co), chromium (Cr), copper (Cu), molybdenum (Mo), nickel (Ni), lead (Pb), antimony (Sb), selenium (Se), vanadium (V) and zinc (Zn) was conducted using an Optima 2100 DV spectrometer (PerkinElmer), following the UNE-EN 15,863 [48]. In the case of the mercury (Hg) present in the eluate a Nippon RA-3 mercury analyser was used (VERTEX), following the UNE-EN ISO 12,846 [49].

3. Results and discussion

Below, the characterization results obtained from the test performed to the MG 7 are shown. The summary of its characteristics and a comparative with the other geothermal grouts is also shown. Moreover, the quantitative improvement entailing the use of nanosilica in the developed geothermal grout is stated.

3.1. MG 7 characterization

As stated above, the thermal conductivity final geothermal grout was 2.01 ± 0.08 W/m•K (K = 2). The results of the 15 essays previously described were:

1. In the flow table a value of 255 mm was obtained, which corresponds to a fluid consistency (greater than200 mm).
2. The initial setting time for the MG 7 was 230 min. The final setting time was 270 min. The room temperature during the test was 20 °C. It can be noted that more than 3 h are available to perform the placement of the geothermal grout.
3. The bleeding of the MG 7 at the end of the test (180 min) was 0.4 %. The temperature of the room during the test was 25 °C.
4. Fresh mortar bulk density: 2.110 kg/m3.
5. Hardened mortar bulk density: 2.046 kg/m^3; Open porosity: 16.7 %.
6. Table 7 shows the average values of the compressive and flexural strength of the MG 7 geothermal grout, obtained after 7 and 28 days respectively.

The MG 7 present high initial strengths, since the compressive and flexural strengths after 7 days, are already 88.6 % and 86.9 % respectively, the strengths after 28 days.

7. In Fig. 11 the two sections of the cylindrical test tubes from the homogeneity study are shown. It is worth noting that the uniformed distribution of the aggregate particles, as it does not display segregation nor anisotropy. The texture of the MG 7 test tube is homogeneous, although there is a small air void (yellow square).

Table 7
Results of the mechanical stress of MG 7.

Compressive strength [N/mm^2]		Flexural strength [N/mm^2]	
7 days	28 days	7 days	28 days
41.9	47.3	5.3	6.1

8. The readings of the linear shrinkage were taken three times. The average result is shown in Fig. 12.

The first reading was done on day 1, *i.e.* the day after the mixing, and immediately after removing the test tubes from the mould. As shown, the linear shrinkage increases considerably during the first 15 days, and then it remains almost constant. The MG 7 has a linear shrinkage of 0.9 mm/m after 90 days.

9. The permeability coefficient determination of the MG 7 is performed with distilled water. A constant pressure gradient of 300 kPa (3 bar) was applied between the test tube extremes. The average value of the 2 tests is $3.2 \cdot 10^{-11}$ m/s, for a water temperature of 20 °C. Hence, it can be concluded that the MG 7 is practically impermeable. IGSHPA (2016) [52]. recommends a permeability coefficient below than 10^{-9} m/s for geothermal grouts.
10. The values of vertical load along with the linear displacements of the coaxial pipe of HDPE were recorded during the adherence test. After 43 min, the maximum vertical load supported by the mortar-pipe was 5.028 kN, with a final displacement of the HDPE coaxial pipe of 2.5 mm. When dividing the load by the lateral area of the HDPE coaxial pipe, a maximum tangential stress of 0.33 N/mm^2 is obtained.
11. After performing the wet-dry and freeze–thaw cycles for the durability test, cracks, fissures, flaking, or peeling were non-existent. The weight loss when these cycles were 3.1 % and 2.1 % respectively. The average values of the compressive and flexural strengths of the reference test tubes and of the test tubes submitted to the freeze–thaw (F-T) and wet-dry (W-D) cycles are shown in Fig. 13.

The MG 7 test tubes that were exposed to wet-dry and freeze–thaw cycles suffered 12.1 % and 10.1 % compressive strength loss, respectively, in relation to the reference test tubes. Equally, the MG 7 test tubes suffered 14.1 % of 10.9 % flexural strength loss after the wet-dry and the freeze–thaw cycles respectively. Therefore, it seems that the MG 7 resists slightly better the freeze–thaw cycles than the wet-dry cycles.

12. Table 8 shows the chemical composition of the main elements of the MG 7 (% in oxides), as well as the trace elements (in mg/kg).

From Table 8, it can be noted that the most abundant elements are silicon (Si) and calcium (Ca). This seems reasonable since the aggregates employed are largely formed by silica. The main cement hydration products are calcium silicate hydrate and calcium hydroxide. It can be observed that the most abundant minor elements existing in the geothermal grout are sulphur (S) and barium (Ba), both come from the barite (barium sulphate) that the mine tailings contain (it is one of the minerals of the gangue). Besides that, sulphur also exists in gypsum, which is added to the cement during its manufacturing process. It is worth noting the high content of some heavy metals (Cu, Ni, Sc, Pb, Zn, Zr, Sr), which they come mainly from the ladle furnace slag (LFS) and fly ash (FA).

13. For the mineralogical analysis, the X-ray generator tube intensity was adjusted to 40 mA, in all measurements. The step size was 0.02° and the step time was 10 s. The crystalline phase identification was executed with the software X'Pert HighScore. The file JCPDS (Joint Committee on Powder Diffraction Standards) was used as a reference file. The main crystalline phases of the MG 7 after 28 days and their relative abundance are shown in Table 9.

It was expected that the most abundant crystalline phase in MG 7 was quartz (SiO_2), as it is the main mineral in the silica sand and in the mine tailings. Portlandite ($Ca(OH)_2$) was formed from the cement hydration

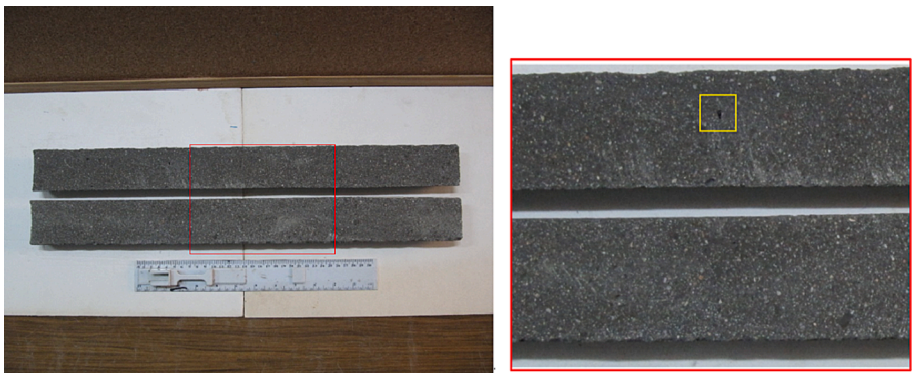

Fig. 11. General view of the section of the cylindrical tubes and detail of the red square. (For interpretation of the references to colour in this figure legend, the reader is referred to the web version of this article.)

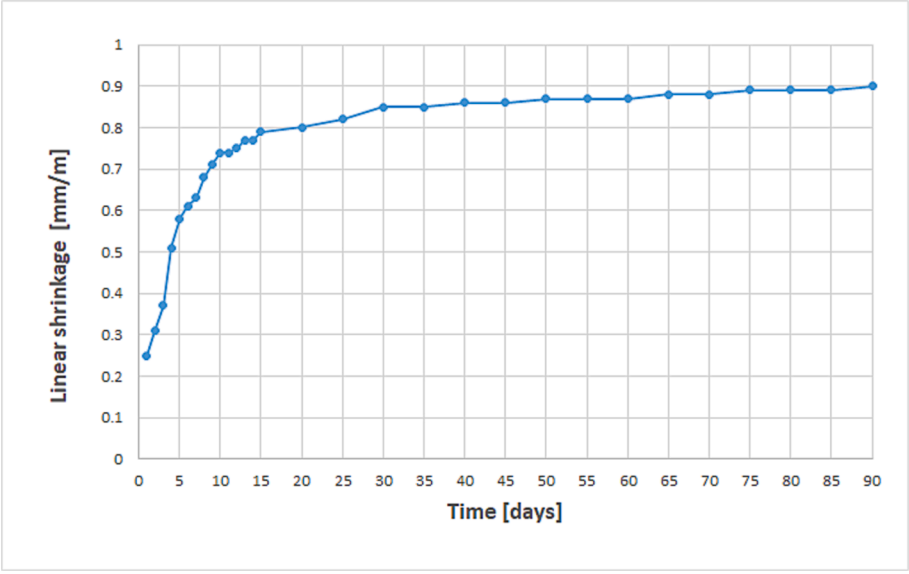

Fig. 12. Results obtained during the linear shrinkage.

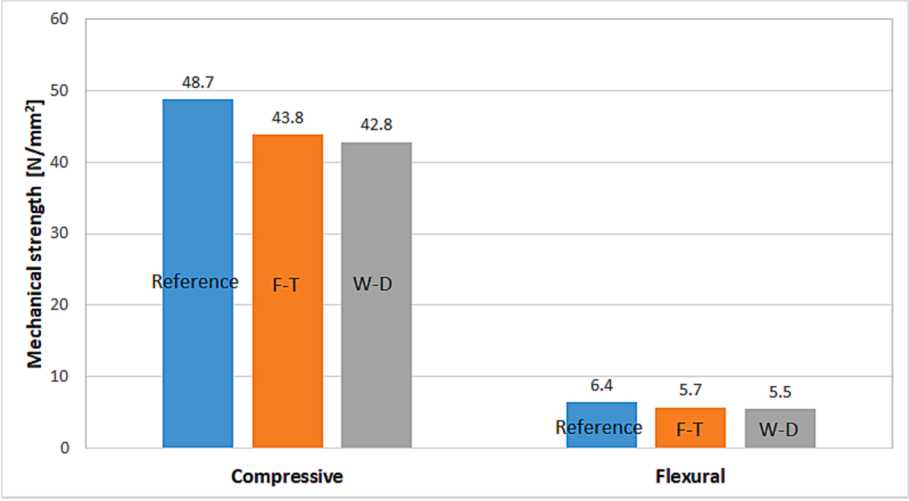

Fig. 13. Comparison of the mechanical strength results.

reactions and it is the second most important hydration product. Calcite ($CaCO_3$) comes mainly from the mine tailings (it is one of the minerals of the gangue) and from the limestone that cement CEM I includes at 5 % maximum proportion. It could also come from the carbonation that the portlandite suffers when it reacts with the carbon dioxide of air. The alite (Ca_3SiO_5) is the main component of the Portland cement clinker.

Table 8
Chemical composition of the MG 7 geothermal grout.

Composition	Content (%)	Element	Content [mg/kg]	Element	Content [mg/kg]
SiO_2	48.80	As	91.96	Zn	508.59
CaO	33.93	Ba	2,779.03	Hg	< LOD
Al_2O_3	3.93	Cd	< LOD	Zr	264.25
Fe_2O_3	2.89	Cr	64.27	Sr	949.53
MgO	1.89	Cu	159.36	Rb	29.72
K_2O	0.35	Mo	26.03	Sc	773.71
TiO_2	0.24	Ni	128.25	Cs	51.30
Na_2O	0.23	Pb	183.06	Te	38.95
MnO	0.07	Sb	35.13	Sn	34.15
LOI	7.23	Se	< LOD	S	4,875.80

LOI: loss on ignition.
LOD: limit of detection.

Table 9
Crystalline phases of the MG 7 geothermal grout after 28 days.

Crystalline phase	Chemical formula	Relative abundance
Quartz	SiO_2	*******
Portlandite	$Ca(OH)_2$	*
Calcite	$CaCO_3$	*
Alite	Ca_3SiO_5	*

Hence, its existence in the hardened mortar is a consequence of the of hydration, and it occurs because after 28 days, the hydration processes speed is not yet completed.

14. In Fig. 14.a, from the SEM image (with secondary electrons) a compact matrix it is observed, although at the centre of the micrograph it is possible to identify a silica sand particle that has a great adherence strength in the aggregate-paste interphase. The same former field was observed with backscattered electrons (Fig. 14.b), highlighting two smaller zones with clearer colours that, from the EDX microanalysis, it was determined that they correspond to two small pyrite crystals. This pyrite comes from the fluorspar tailings (FT).
15. In Table 10, it is possible to observe pH and electrical conductivity values of the eluates collected in the 4 stages of the leaching test (after 3, 7, 30 and 60 days). These values correspond to a water temperature of 25 °C.

Even though the pH decreased, after 60 days was still high. The alkalinity comes mainly from the portlandite (calcium hydroxide), formed during the setting and hardening of the cement. It can be observed that the leachate has a relatively low electrical conductivity,

Table 10
pH and electrical conductivity of the eluate collected after 3, 7, 30 and 60 days respectively.

	3 days	7 days	30 days	60 days
pH	11.98	11.43	11.09	10.84
Electrical conductivity [μS/cm]	2.0132	1.983	1.764	1.516

even in the collected water in the first stage (after 3 days). The Royal Decree 140/2003 [50] fixes a maximum value of 2,500 μS/cm for human consumption water.

The eluate collected in the last stage (after 60 days) had a turbidity of 3.5 NTU (Nephelometric Turbidity Units). Royal Decree 140/2003 fixes a maximum value of 5 NTU for human consumption water.

To estimate the chemical composition of the collected eluate in the last stage, twelve chemical elements were analysed. Table 11 shows the obtained results, as well as the maximum values established by the Royal Decree 140/2003 [50] and WHO (2011) [51], for human consumption waters.

It can be noted that many of the elements in the MG 7 had not leached, which indicates that they were retained in the cementitious matrix, mainly due to the low permeability of the MG 7. Moreover, the released elements presented low concentrations (<4 μg/l), except for Barium (Ba) that had a high value due to its greater abundance and solubility. It is shown that the concentration of harmful elements in the eluate is lower than the established maximum (Royal Decree 140/2003 [50] and WHO 2011 [51]). Therefore, it can be concluded that the MG 7 does not affect

Table 11
Concentration of elements leached from MG 7 after 60 days and maximum values.

Element	Concentration [μg/l]	Maximum value [μg/l]
As	3.196	10
Ba	668.123	700*
Cd	< 1	5
Cr	1.621	50
Hg	< 1	1
Mo	1.476	70*
Ni	< 1	20
Pb	< 1	10
Sb	< 1	5
Cu	3.556	2,000
Se	< 1	10
Zn	2.365	3.000*

* Stablished values by WHO (2011) [51].

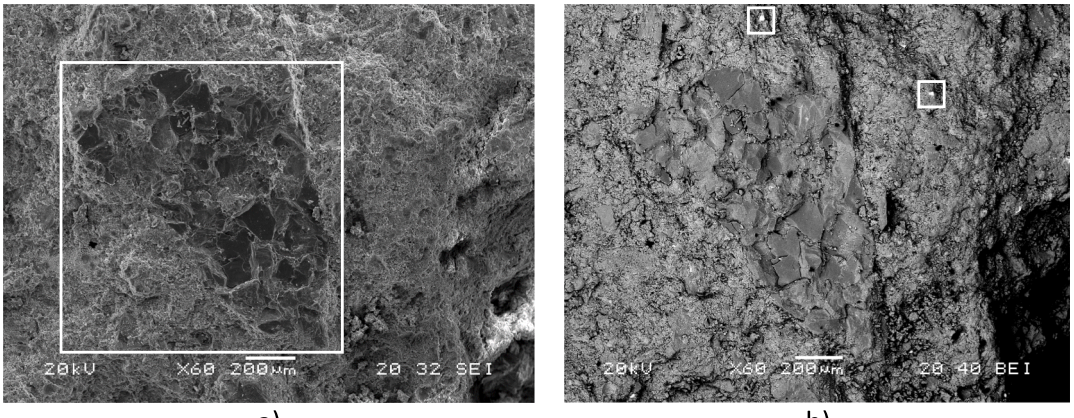

Fig. 14. Micrograph of the MG 7. a) Matrix and silica sand particle. b) Pyrite crystals.

3.1.1. Summary of MG 7 characteristics

A summary of MG 7 characteristics is shown in Table 12.

3.2. Comparative study of MG 7 with other geothermal grouts

Table 13 shows the thermal conductivity in dry conditions, the coefficient of permeability and compressive strength, after 28 days, of the MG 7, Mix 111 and of 6 geothermal commercial grouts. The Mix 111 geothermal grout was developed by Allan and Philippacopoulos., 1999 [44]. This geothermal grout was approved by the New Jersey Department of Environmental Protection and it was successfully employed in many commercial projects in the USA.

Comparing MG7 and Mix 11, it can be concluded that both have very similar thermal conductivity. However, the MG 7 geothermal grout has a greater compressive strength but lower coefficient of permeability. Comparing MG 7 with the 6 commercial geothermal grouts, it is shown that only the EnerGrout HD 2.1 exceeds slightly MG 7 thermal conductivity. The other properties present better values in the MG 7 than in the 6 commercial geothermal grouts.

3.3. Nanosilica contribution to the improvement of the properties

To quantify the influence of the nanosilica in the main properties of the MG 7, in additional, a geothermal grout (MG 8) was developed. MG 8 had the same materials and mix proportions as the MG 7, except for the nanosilica. The results obtained in the three most important properties of a geothermal grout are shown in Table 14.

The difference between both geothermal grouts is: 9.95 % in thermal conductivity; 15.63 % in the permeability coefficient and 12.47 % in the compressive strength on the day 28.

4. General conclusions

This article shows the process to make an optimal geothermal grout, according to its thermal properties. For this, it started from mining, metallurgy and energetic industries waste from the surroundings of the University where the study was developed. The selected waste, with low commercial value, have properties which improve the geothermal grout ones. In the first phase 30 samples were prepared and were subject to quality analysis about workability, exudation, cracking, simple compressive strength, etc. After this analysis, the optimal 7 samples were selected. To these 7 samples, a thermal assay had been done where the optimal sample was MG7 because it has the best balance between the value of thermal conductivity and the percentage of artificial aggregates. This thermal analysis was performed with a device designed, built and calibrated by the authors. Regarding the properties of the selected grout, the following conclusions were reached:

MG 7 is a dry mortar (pre-dosed geothermal grout), where 30 % of the aggregates are artificial (10 % fluorspar tailings, 10 % ladle furnace slag, 7 % fly ash and 3 % silica fume). The rest of the components of the mortar are Portland cement, silica sand, 2 % powdered nanosilica and powdered superplasticizer.

The materials and tests performed for the characterization development of a cement-based geothermal grout named MG 7 are shown. The following types of properties have been considered: thermal, mechanical, physical, and environmental properties, as well as the recovery of aggregates, and the availability and costs of the employed materials.

- To date, nanosílice has not been used as geothermal backfill material.
- 10 % of fluorspar tailings and 10 % of ladle furnace slag were employed in the MG 7 formulation. Since fluorspar tailings have no commercial application and ladle furnace slag barely has it, the use of both in geothermal grouts is noteworthy.
- The use of 2 % of nanosilica in the MG 7 provides approximately 10–15 % improvement in the three main properties of a geothermal grout: thermal conductivity, permeability, and compressive strength.
- The MG 7 has a thermal conductivity of 2.01 $\pm$ 0.08 W/m•K (K = 2). This value is greater than most of the commercial geothermal grouts. The mechanical strength and permeability values of the MG 7 are better than those of the commercial geothermal grouts.
- The MG 7 presents negligible values of bleeding after 3 h and linear shrinkage after 90 days. During the homogeneity study of the geothermal grout, it was proven that it does not have anisotropy nor segregation.
- The MG 7 geothermal grout has an initial setting time greater than 3 h, sufficient for placing the grout in a BHE. Moreover, the fluid consistency of the MG 7 makes it appropriate for injection in the BHE.
- The MG 7 geothermal grout has shown good behavioural characteristics in the freeze–thaw and wet-dry cycles respectively, with an

Table 12
Characteristics of the MG 7 geothermal grout.

Type of geothermal grout	Dry mortar (pre-dosed)
Materials	Portland cement (CEM I 42,5 R) Silica sand from quarry Fluorspar tailings Fly ash from pulverized coal power plants Ladle furnace slag Silica fume Nanosilica Superplasticizer
Mixing water	1 L for each 6 kg of dry mortar
Maximum grain size	2 mm
Artificial aggregate percentage	30 %
Consistency	Fluid (255 mm in the flow table)
Initial setting time	230 min
Final setting time	270 min
Bleeding (after 3 h)	0.4 %
Fresh mortar density	2,110 kg/m^3
Hardened mortar density	2,046 kg/m^3
Open porosity	16.7 %
Compressive strength (after 7 days)	41.9 N/mm^2
Compressive strength (after 28 days)	47.3 N/mm^2
Flexural strength (after 7 days)	5.3 N/mm^2
Flexural strength (after 28 days)	6.1 N/mm^2
Linear shrinkage (after 90 days)	0,9 mm/m
Coefficient of permeability	$3.2{\cdot}10^{-11}$ m/s
Thermal conductivity	2.01 W/m•K

Table 13
Comparison of MG 7 with other geothermal grouts.

Name	Thermal conductivity [W/m•K]	Coefficient of permeability [m/s]	Compressive strength [N/mm^2]
MG 7	2.01	$3.2{\cdot}10^{-11}$	47.3
Mix 111	2.16	$1.6{\cdot}10^{-12}$	36.7
MASTEC® Geotérmico	1.70	$1.0{\cdot}10^{-10}$	5.0
ERKAN GEO	1.80	$1.5{\cdot}10^{-10}$	6.1
EnerGrout HD 2.1	2.10	$1.0{\cdot}10^{-10}$	3.0
PROPAM® GEOTHERM	1.90	$3.0{\cdot}10^{-10}$	10.0
GWE Thermokontakt®	1.30	$1.0{\cdot}10^{-9}$	3.0
ThermoCem®PLUS	2.00	$1.0{\cdot}10^{-10}$	6.0

Table 14
Results obtained with nanosilica (MG 7) and without nanosilica (MG 8).

Name	Thermal conductivity [W/m•K]	Coefficient of permeability [m/s]	Compressive strength [N/mm^2]
MG 7	2.01	$3.2{\cdot}10^{-11}$ m/s	47.3
MG 8	1.81	$3.7{\cdot}10^{-11}$ m/s	41.4

insignificant weight loss percentage and mechanical strength and with no fissures, cracks, flaking or peeling.
- The MG 7 is environmentally safe. The physical and chemical parameters analysed in the eluate fulfil the Royal Decree 140/2003 [50] and the maximum values fixed by WHO (2011) [51] for waters intended for human consumption.

Thus, after an exhaustive selection of materials, mix proportions, and physical, thermal, mechanical, mineralogical, chemical and microstructural characterization, it can be concluded that the MG 7 geothermal grout satisfies all the requirements. Hence, its properties are appropriate for being employed in a BHE. Moreover, MG 7 geothermal grout is economical, and the materials employed are available in the area in which the research is developed.

CRediT authorship contribution statement

C. Castán-Fernández: Investigation, Supervision, Writing – review & editing, Data curation. **G. Marcos-Robredo:** Investigation, Data curation. **M.P. Castro-García:** Investigation, Supervision, Writing – review & editing. **M.A. Rey-Ronco:** Investigation, Data curation, Supervision. **T. Alonso-Sánchez:** Investigation, Supervision, Writing – review & editing.

Declaration of Competing Interest

The authors declare that they have no known competing financial interests or personal relationships that could have appeared to influence the work reported in this paper.

Data availability

Data will be made available on request.

Acknowledgments

Authors wish to thank the financial support provided by the FICYT (Government of the Principality of Asturias) with reference BP14-074 and the Cátedra HUNOSA.

We wish to thank the research group of the Cátedra Hunosa of the University of Oviedo, in particular Laura Cordero Llana; Teresa Fernández González; Saúl Norniella Llaneza and Marina del Riego Nozal for editing and translating the article.

The authors would also like to thank the Minersa Group, the Hunosa Group, Cantera Grado S.L., the Masaveu Group, Juan Tapia España and Marta Fernández Gómez for their collaboration.

References

[1] A.J. Philippacopoulos, M.L. Berndt, Influence of debonding in ground heat exchangers used with geothermal heat pumps, Geothermics 30 (5) (2001) 527–545.
[2] L. Jin, X. Wei, H. Tao, X. Wei, R. Joachim, Thermo-economic analysis of borehole heat exchangers (BHE) grouted using drilling cuttings in a dolomite area, Appl. Therm. Eng. 150 (2019) 305–315.
[3] I. Indacoechea Vega, P. Pascual Muñoz, D. Castro Fresno, M.A. Calzada Pérez, Experimental characterization and performance evaluation of geothermal grouting materials subjected to heating–cooling cycles, Constr. Build. Mater. 98 (2015) 583–592.
[4] C. Sáez Blázquez, A. Farfán Martín, I. Martín Nieto, P. Carrasco García, L. S. Sánchez Pérez, D. González-Aguilera, Analysis and study of different grouting materials in vertical geothermal closed-loop systems, Renewable Energy 114 (2017) 1189–1200.
[5] Hellström, G. (2011). Chapter 6: Borehole Heat Exchangers. Geotrainet Training Manual for Designers Shallow Geothermal Systems. Brussels: Dr. Maureen Mc Corry with EurGeol. Gareth Ll. Jones.
[6] Allan, M.L. (2015). Quality Control and Troubleshooting for Grouts Used with Geothermal Heat Pumps. World Geothermal Congress, Melbourne, 2015.
[7] K. Daehoon, K. Gyoungman, K. Donghui, B. Hwanjo, Experimental and numerical investigation of thermal properties of cement-based grouts used for vertical ground heat exchanger, Renewable Energy 112 (2017) 260–267.
[8] J. Côté, J.-M. Konrad, A generalized thermal conductivity model for soils and construction materials, Can. Geotech. J. 42 (2) (2005) 443–458.
[9] R. Borinaga-Treviño, P. Pascual-Muñoz, D. Castro-Fresno, J.J. Del Coz-Díaz, Study of different grouting materials used in vertical geothermal closed-loop heat exchangers, Appl. Therm. Eng. 50 (1) (2013) 159–167.
[10] Sanner, B. (2011). Chapter 4: Ground Heat Transfer. *Geotrainet training manual for designers shallow geothermal systems*. Brussels: Dr. Maureen Mc Corry with EurGeol. Gareth Ll. Jones.
[11] C. Lee, K. Lee, H. Choi, H.-P. Choi, Characteristics of thermally-enhanced bentonite grouts for geothermal heat exchanger in South Korea, Sci. China Technol. Sci. 53 (1) (2010) 123–128.
[12] B. Sanner, C. Karytsas, D. Mendrinos, L. Rybach, Current status of ground source heat pumps and underground thermal energy storage in Europe, Geothermics 32 (4-6) (2003) 579–588.
[13] K. Young Sang, D. Ba Huu, D. Tan Manh, O. Gyeong, K., Development of thermally enhanced controlled low-strength material incorporating different types of steel-making slag for ground-source heat pump system, Renewable Energy 150 (2020) 116–127.
[14] UNE-EN 1015-6:1999. Methods of test for mortar for masonry - Part 6: Determination of bulk density of fresh mortar. AENOR.
[15] S. Erol, B. François, Efficiency of various grouting materials for borehole heat exchangers, Appl. Therm. Eng. 70 (1) (2014) 788–799.
[16] P. Pascual Muñoz, I. Indacoechea Vega, D. Zamora Barraza, D. Castro Fresno, Experimental analysis of enhanced cement-sand-based geothermal grouting materials, Constr. Build. Mater. 185 (2018) 481–488.
[17] Allan, M.L., Philippacopoulos, A.J. (2000). Performance Characteristics and Modelling of Cementitious Grouts for Geothermal Heat Pumps. World Geothermal Congress, Tohoku, 2000.
[18] M. Montaser, R. Mohamad, P. Keith, A.A. Mohammad, W. Tabbi, O. Abdul, N. Sumsun, A review of grout materials in geothermal energy applications, Internat. J. Thermofluids 10 (2021), 100070.
[19] P.K. Dehdezi, M.R. Hall, A.R. Dawson, Enhancement of soil thermo-physical properties using microencapsulated phase change materials for ground source heat pump applications, Appl. Mech. and Mater. 110–116 (2011) 1191–1198.
[20] Allan, M.L. (1996). Preliminary Study on Improvement of Cementitious Grout Thermal Conductivity for Geothermal Heat Pump Applications. Informal Report, BNL 63195. Brookhaven National Laboratory.
[21] M.L. Allan, S.P. Kavanaugh, Thermal conductivity of cementitious grouts and impact on heat exchanger length design for ground source heat pumps, Internat. J. HVAC&R Res. 5 (2) (1999) 87–98.
[22] M.L. Berndt, A.J. Philippacopoulos, Incorporation of fibres in geothermal well cements, Geothermics 31 (6) (2002) 643–656.
[23] M.L. Allan, Thermal conductive of cementitious grouts for geothermal heat pumps. FY 1997 progress report, BNL 65129, Brookhaven National Laboratory, 1997.
[24] M.L. Berndt, Strength and permeability of steel fibre reinforced grouts, Constr. Build. Mater. 24 (9) (2010) 1768–1772.
[25] R. Borinaga-Treviño, P. Pascual-Muñoz, D. Castro-Fresno, E. Blanco-Fernandez, Borehole thermal response and thermal resistance of four different grouting materials measured with a TRT, Appl. Therm. Eng. 53 (1) (2013) 13–20.
[26] K. Young Sang, D. Tan Manh, K. Min Jun, K. Bong Ju, K. Hyeong Ki, Utilization of by-product in controlled low-strength material for geothermal systems: Engineering performances, environmental impact, and cost analysis, J. Cleaner Prod. 172 (2018) 909–920.
[27] D. Tan Manh, K. Hyeong Ki, K. Min Jun, K. Young Sang, Utilization of controlled low strength material (CLSM) as a novel grout for geothermal systems: Laboratory and field experiments, J. Build. Eng. 29 (2020), 101110.
[28] F. Delaleux, X. Py, R. Olives, A. Dominguez, Enhancement of geothermal borehole heat exchangers performances by improvement of bentonite grouts conductivity, Appl. Therm. Eng. 33–34 (2012) 92–99.
[29] A.A. Alrtimi, M. Rouainia, D.A.C. Manning, Thermal enhancement of PFA-based grout for geothermal heat exchangers, Appl. Therm. Eng. 54 (2) (2013) 559–564.
[30] K. Dequan, W. Rong, C. Jianxun, K. Jiayuan, J. Xintong, Effect of gradation on the thermal conductivities of backfill materials of ground source heat pump based on loess and iron tailings, Appl. Therm. Eng. 180 (2020), 115814.
[31] W.D. Callister, Introducción a la ciencia e ingeniería de los materiales 2, Editorial Reverte S.A, Barcelona, 2007.
[32] UNE-EN 993-1:1996 Methods of test for dense shaped refractory products - Part 1: Determination of bulk density, apparent porosity and true porosity. AENOR.
[33] ISRM (1981). The ISRM Suggested Methods for Rock Characterization, Testing and Monitoring: 2007-2014.
[34] ASTM C940-98a. Standard Test Method for Expansion and Bleeding of Freshly Mixed Grouts for Preplaced-Aggregate Concrete in the Laboratory.
[35] Castán-Fernández C.; Marcos-Robredo G.; Rey-Ronco M.A.; Alonso-Sánchez T. (2018). Design, Construction and Commissioning of an Apparatus for Measuring the Thermal Conductivity of Geothermal Grouting Materials Based on the Transient Hot Wire Method. Proceedings, *2*(23), 1496; https://doi.org/10.3390/proceedings2231496.
[36] UNE-EN 1015-2:1999. Methods of test for mortar for masonry - Part 2: Bulk sampling of mortars and preparation of test mortars. AENOR.
[37] UNE-EN 1015-3:2000. Methods of test for mortar for masonry - Part 3: Determination of consistence of fresh mortar (by flow table). AENOR.
[38] UNE-EN 480-2:2007. Admixtures for concrete, mortar and grout - Test methods - Part 2: Determination of setting time. AENOR.
[39] UNE-EN 1015-6:1999. Methods of test for mortar for masonry - Part 6: Determination of bulk density of fresh mortar.

[40] UNE-EN 1015-10:2000. Methods of test for mortar for masonry - Part 10: Determination of dry bulk density of hardened mortar. AENOR.
[41] UNE-EN 1015-11:2000. Methods of test for mortar for masonry - Part 11: Determination of flexural and compressive strength of hardened mortar. AENOR.
[42] ASTM C490-07. Standard Practice for Use of Apparatus for the Determination of Length Change of Hardened Cement Paste, Mortar, and Concrete.
[43] ASTM D5084-90. Standard Test Methods for Measurement of Hydraulic Conductivity of Saturated Porous Materials Using a Flexible Wall Permeameter.
[44] M.L. Allan, A.J. Philippacopoulos, Properties and performance of cement-based grouts for geothermal heat pump applications, Final report. (1999).
[45] UNE-EN ISO 10523:2012. Water quality - Determination of pH. AENOR.
[46] UNE-EN ISO 7027-1:2016. Water quality - Determination of turbidity - Part 1: Quantitative methods. AENOR.
[47] UNE-EN ISO 11885:2010. Water quality - Determination of selected elements by inductively coupled plasma optical emission spectrometry (ICP-OES). AENOR.
[48] UNE-EN 15863:2015. Characterization of waste. Leaching behaviour test for basic characterization - Dynamic monolithic leaching test with periodic leachant renewal, under fixed conditions. AENOR.
[49] UNE-EN ISO 12846:2012. Water quality - Determination of mercury - Method using atomic absorption spectrometry (AAS) with and without enrichment. AENOR.
[50] Royal Decree 140/2003 of 7 February by which health criteria for the quality of water intended for human consumption are established. B.O.E Number: 45/2003; Publication date: 21/02/2003.
[51] WHO, Guidelines for drinking-water qualit, fourth ed., World Health Organization, 2011.
[52] IGSHPA, Closed-Loop/Geothermal Heat Pump Systems Design and Installation Standards, Oklahoma State University, 2016.